Published in J. Electronic Materials 30, 162 (2001).

Properties of GaN epitaxial layers grown on 6H-SiC(0001) by plasma-assisted molecular beam epitaxy

C. D. Lee, V. Ramachandran, Ashutosh Sagar, and R. M. Feenstra
Department of Physics, Carnegie Mellon University, Pittsburgh, Pennsylvania 15213
D. W. Greve
Department of Electrical and Computer Engineering, Carnegie Mellon University, Pittsburgh, PA 15213
W. L. Sarney and L. Salamanca-Riba
Materials and Nuclear Engineering Department, University of Maryland, College Park, MD 20742-2115
D. C. Look
Wright State University and Air Force Research Laboratory, Dayton, Ohio 45435
Song Bai, W. J. Choyke and R. P. Devaty
Department of Physics and Astronomy, University of Pittsburgh, Pittsburgh, Pennsylvania 15260

Abstract

The structural, electrical, and optical properties of GaN grown on 6H-SiC(0001) substrates by molecular beam epitaxy are studied. Suitable substrate preparation and growth conditions are found to greatly improve the structural quality of the films. Threading dislocation densities of about 1×10^9 cm^{-2} for edge dislocations and $< 1 \times 10^6$ cm^{-2} for screw dislocations are achieved in GaN films of 0.8 μm thickness. Mechanisms of dislocation generation and annihilation are discussed. Increasing the Ga to N flux ratio used during growth is found to improve the surface morphology. An unintentional electron concentration in the films of about 5×10^{17} cm^{-3} is observed, and is attributed to excess Si in the films due to a Si-cleaning step used in the substrate preparation. Results from optical characterization are correlated with the structural and electronic studies.

1 Introduction

The large band gap, high breakdown field, and high electron saturation velocity of GaN make it ideal for use in visible-to-UV optoelectronic devices and high speed, high power electronic applications. Almost all such devices developed over the past number of years have been fabricated in material grown by metalorganic chemical vapor deposition (MOCVD). Unfortunately, bulk GaN in wafer sizes is not available, so most growth is performed on sapphire. Despite a lattice mismatch to GaN of about 14%, MOCVD growth on sapphire using an appropriate low-temperature buffer layer yields relatively high quality material. Dislocation densities as low as 7×10^8 cm^{-2} for threading dislocations which intersect the surface have been reported [1]. The recent innovation of lateral epitaxial overgrowth leads to a reduction in this density by several orders of magnitude in the laterally grown regions of the films [2,3], but the process is somewhat complicated. An alternate sub-

strate is SiC, with 3.4% mismatch to GaN. Early work with this material yielded results which were no better than those using sapphire, although recently with the use of H-etching of SiC to improve its surface morphology growth of GaN on SiC by molecular beam epitaxy (MBE) has demonstrated material of relatively high quality, suitable for device applications [4-9].

In this work we report on structural, electrical, and optical characteristics of MBE grown GaN on SiC. Details are given of H-etching and Si-cleaning steps used on the SiC substrates prior to growth. The evolution of the film morphology is monitored using atomic force microscopy (AFM) and scanning tunneling microscopy (STM). Dislocations in the film are characterized using transmission electron microscopy (TEM) and high resolution x-ray diffraction (HRXRD), yielding a detailed picture of the dislocation generation and annihilation in the films. We distinguish between high temperature and low temperature growth regimes, $\gtrsim 650^\circ$ C or $\lesssim 600^\circ$ C respectively, in discussing the results. Electrical characterization reveals the presence of substantial unintentional doping in the material, which is attributed to the presence of Si (arising from the Si-cleaning step) as seen in secondary-ion mass spectrometry (SIMS). Low-temperature photoluminescence (PL) provides information on the point defect concentration in the films and reveals cubic inclusions in non-optimally prepared material.

2 Experimental

GaN films of typically 0.8 μm thickness are deposited by MBE on Si-face on-axis 6H-SiC(0001) substrates. Activated nitrogen is supplied by an SVTA RF-plasma source, and effusion cells are used for Ga and various dopants. Ultra-high purity (99.9999%) nitrogen is used. It is passed through an Aeronex gas purifier (except for some of our early films, where this purifier was not installed) which we find from residual gas analysis is effective at removing oxygen and water from the source gas. Ga fluxes are measured with a crystal thickness monitor, and the active N flux is calibrated by defining the Ga/N flux ratio to be unity at the point where a transition between streaky and spotty behavior occurs in the reflection high energy electron diffraction (RHEED) pattern [10,11]. Hydrogen etching of the SiC is carried out at a temperature of 1600–1700° C with a hydrogen flow of about 14 liters/min [4]. The H-etching produces a surface with steps of only half or full unit cell height (7.5 or 15 Å for 6H-SiC). As discussed in Section IV, we feel that the 6H polytype of SiC is best for GaN epitaxy since these step heights then prevent the formation of stacking mismatch boundaries [6] which would be encountered for either unetched SiC or 4H material. Following H-etching, the SiC substrates are transferred through air to the MBE chamber. Prior to deposition, the samples are first outgassed at about 800° C for 30 minutes. To remove the surface oxide formed during transfer through air, several monolayers of Si are deposited on the substrate while it is near room temperature. It is then annealed at 1000° C and the RHEED pattern is monitored. It starts at 3×3, then changes to 1×1, and then forms a 3×1 pattern after about an hour of annealing. This latter pattern is indicative of a $\sqrt{3} \times \sqrt{3}$-R30° surface reconstruction, a structure which is known to consist of 1/3 monolayer (ML = 1.22×10^{15} atoms/cm^2) of Si adatoms on top of a bulk-terminated SiC bilayer [12].

X-ray measurements are performed in the triple-crystal configuration, using Cu α_1 radiation. TEM is done using a JEOL 4000FX operating at 300 kV. Anisotropic etching to reveal dislocations is done using 0.03 M KOH and focused illumination from a Hg arc lamp [13]. Comparison of dislocation density from the etching technique with that from TEM was performed for MOCVD-grown GaN, and good agreement was obtained between the two methods [14]. PL is per-

formed at a temperature of 2 K, usually using a frequency doubled Ar ion laser producing 244 nm excitation. In specific cases, as noted below, a He-Cd laser operating at 325 nm is used to provide a longer absorption length for the excitation.

3 Morphological Evolution During Growth

AFM images reveal that the H-etched SiC substrates consist of shallow facets, with facet angles less than the unintentional miscut of the wafer [4]. On a single facet all steps are found to have full unit cell height, and the steps have normal vectors directed in a $<1\bar{1}00>$ direction [4]. A neighboring facet has step normals directed in another $<1\bar{1}00>$ direction, rotated 60° from the first, and the terraces on that facet are then half a unit cell offset in height from those of the first. Consequently, half unit cell high steps occur at the intersections of the facets. The Si-cleaning procedure described in Section II, used to remove the surface oxide, modifies the surface morphology of the SiC. Figure 1 shows an AFM image obtained after this Si-cleaning step. The morphology is seen to consist of terraces, which are in this case separated by half unit cell high (7.5 Å) steps. Near the top of the image the steps form pairs, and it is apparent that they have formed from full unit cell high steps. The Si-cleaning step has apparently produced some etching of the SiC (in addition to removing the oxide which formed on the surface). The small hexagonal holes seen in the terraces of Fig. 1 have depth of half a unit cell. Further etching causes them to merge with the step leading to the lower terrace, and the step edge then acquires a very irregular shape. One subtle feature which is barely visible in Fig. 1 is that the contrast on the terraces themselves is slightly irregular, suggesting some nonuniformity of the terraces. STM imaging of the same sample revealed that the surface contained a mixture of 3×3 and $\sqrt{3} \times \sqrt{3}$-R30° surface reconstructions, thus illustrating a problem with the Si-cleaning method in that the precise Si coverage (1/3 ML) cannot always be precisely obtained.

Following the Si-cleaning of the SiC, MBE growth is initiated by simultaneously exposing the substrate to the N and Ga fluxes. Figure 2 shows STM results for the morphology of a 0.3 ML thick film, with the deposition performed at 650° C. Nucleation of the film is seen to occur randomly on the SiC terraces. The evolution of the film morphology varies with growth temperature. For high temperature (HT) growth, $\gtrsim$ 650° C, the GaN grows as flat-topped 3-dimensional islands [5]. At film thickness of 4 nm the islands have *not* coalesced, whereas we expect from an estimated critical thickness of 2–3 nm that the strain in the GaN has relaxed at that film thickness [15]. As discussed in Section IV, the dislocations which produce this strain relaxation have Burgers vector $\mathbf{b} = 1/3 <11\bar{2}0>$, and for thicker films the threading dislocations they give rise to all have that same character (*i.e.* edge dislocations). In contrast, for low temperature (LT) growth, $\lesssim$ 600° C, the GaN film at 4 nm thickness completely wets the SiC substrate [5]. This film is strain relaxed by the formation of a network of dislocations which give rise to threading dislocations with *both* edge and screw character, as well as possibly some mixed character threading dislocations.

For thicker films, the resulting morphology reflects the dislocation content of the films. For LT growth, screw (or mixed) character threading dislocations give rise to spiral growth features, as previously presented [5]. HT films display very few spiral growth features since they contain very few screw dislocations. The film morphology is also found to depend on the Ga/N flux ratio, as shown in Fig. 3. For moderately Ga-rich conditions, with Ga/N flux ≈ 1.3, we find relatively flat films interspersed with small pits as shown in Fig. 3(a). The rms roughness for that image is 2.9 nm, and in regions between the pits the rms roughness is 0.5 nm. From a number of cross-sectional TEM images we find a correlation of the pit location and the presence of a threading dislocation.

We thus tentatively attribute the pit formation with some sort of equilibrium pit structure near dislocations or perhaps with the decomposition of the GaN during growth near the dislocation. For lower flux ratios ≈ 1.1 the size and number of pits grows, and they often merge to form trenches, as in Fig. 3(b). Finally, for higher flux ratios ≈ 1.6 the pit formation is inhibited, as shown in Fig. 3(c). In that case, however, Ga droplets start to form on the surface as seen by visual inspection of the films.

4 Structural Characterization

TEM results for an optimized HT growth are shown in Fig. 4; panels (a) and (b) show the two-beam images which are sensitive to threading edge and screw dislocations, respectively [16]. A high density of edge dislocations is seen near the GaN/SiC interface, and these dislocations are seen to reduce their number significantly by annihilation as one moves to the surface of the film. The density of threading edge dislocations at the surface is found to be $\approx 3 \times 10^9$ cm^{-2}, and similar values are found in other samples. These values are higher than our previously reported density of 2×10^8 cm^{-2} [16,17]; some uncertainty in this lower value exists since some of the dislocations in that film terminated in surface pits (rather than the surface plane) and were not counted. Consequently the 2×10^8 cm^{-2} value is perhaps an underestimate, and a better value for that earlier sample is about 8×10^8 cm^{-2}. We have used anisotropic etching and plan view scanning electron microscopy (SEM) to obtain a more accurate count of dislocation density. Results are shown in Fig. 5, where each protrusion arises from a single dislocation or a small group of dislocations. For the groups of dislocations, close examination of the image generally allows one to estimate the number of dislocations in each group. Counting the dislocation density from this and other images we arrive at a value of 6×10^8 cm^{-2}. Combining the SEM and TEM results, we estimate our edge dislocation density to be about 1×10^9 cm^{-2}.

Concerning threading screw dislocations, none are observed in Fig. 4(b) nor on neighboring regions of the film that were imaged by TEM. Similar results were obtained from other samples. From these results we can set an upper bound of $< 1 \times 10^8$ cm^{-2} for the screw dislocation density. A more stringent limit can be obtained by examination of AFM images such as those shown in Fig. 3. Screw dislocations lead to growth spirals, which are easily seen in AFM images [5]. For the case of HT optimized growth such as that shown in Fig. 3, we observe no growth spirals in an imaged surface area of $> 10^{-6}$ cm^2, leading to a threading screw dislocation density at the surface of $< 1 \times 10^6$ cm^{-2}.

High resolution TEM images are shown in Fig. 6, for HT-growth material, with and without H-etching. The H-etched material shows a well defined interface, with no apparent steps, and the GaN film has perfect hexagonal (wurtzite) stacking. In contrast, the film grown on the non-H-etched substrate shows thin regions of cubic (zincblende) stacking near the interface; these films also show dislocation densities much higher than those obtained using H-etching. We interpret the formation of the cubic stacked regions as arising from single bilayer steps present on the non-H-etched material, which leads to nonideal stacking as previously discussed by Torres *et al.* [6] and illustrated in Fig. 7. Each bilayer of GaN on SiC can be assigned a direction, right (R) or left (L), as given *e.g.* by the direction of a N atom from a neighboring Ga (or a C atom from a Si). For the hexagonal stacking of GaN the plane orientations alternate as RLRLRL..., for 4H-SiC the orientations are RRLLRRLL..., and for 6H-SiC they are RRRLLLRRRLLL.... If a step occurs in the SiC substrate (4H or 6H) between LL or RR bilayers, as pictured in Fig. 7, then the GaN grains growing

on the two terraces will have opposite orientation. Overgrowth of one grain by the other is expected to produce regions of cubic stacking in the GaN as well as the formation of stacking faults at the junction between the cubic and hexagonal stacked material. Half unit cell high steps of 4H-SiC will also lead to such stacking defects. Full unit cell high steps of 4H or 6H-SiC, or half unit cell high steps of 6H-SiC, will *not* produce the stacking defects.

In addition to TEM analysis, the structural quality of our films has been characterized by HRXRD. Table I shows average results for a number of films grown near 750° C, compared to those of other groups. Our results are comparable to those of Brandt *et al.* [9] who use similar substrate preparation and growth methods. Similarly, these MBE results compare favorably with the results for MOCVD growth on sapphire of Heying *et al.* [1]. (Different asymmetric reflections were measured by the groups listed in Table I, although the values can be scaled in a manner following Fig. 8 of Ref. [18]). Our asymmetric ω-2θ width is somewhat greater than that of Heying *et al.*, but the symmetric and asymmetric ω-scan widths are significantly less than theirs and the density of screw dislocations determined for our samples is much lower than that for the MOCVD on sapphire growth. Recent theoretical work indicates that edge dislocations may be preferable compared to screw dislocations since, at least for full core dislocations, the latter do have states in the gap whereas the former do not [19].

5 Electrical Characterization

Temperature dependent conductivity and Hall effect measurements have been performed on GaN films grown on semi-insulating SiC substrates. For all our films grown with the *in situ* Si-cleaning step described in Section II we find a relatively high background n-type carrier concentration, typically 5×10^{17} cm^{-3} at room temperature. This value is derived assuming that the carriers are uniformly distributed throughout the entire GaN film. Typical electron mobilities of about 50 cm^2/Vs are observed at room temperature. When the temperature is reduced down to 13 K we find that the apparent carrier concentration does *not* decrease significantly (it actually increases slightly) as would be expected for carrier freeze-out onto the donor impurities, indicating that the room temperature carrier concentration must be indicative of conductance through a much thinner region. That is, the actual electron concentration must be significantly greater than 10^{18} cm^{-3} in order to produce the degenerate electrical behavior, and thus the thickness of this highly doped layer must be less than the total layer thickness.

SIMS measurements have been performed on the GaN films in an effort to identify the possible source of the background donors. Carbon and oxygen concentrations are found to be below the sensitivity of the SIMS, which is 1×10^{17} cm^{-3} and 2×10^{17} cm^{-3} for those elements respectively. Si is consistently observed in the films at a level of around 1×10^{18} cm^{-3}, although the Si concentration varies by about an order of magnitude from film to film and also shows considerable variation at different locations within the same film. A typical SIMS profile is shown in Fig. 8. A Si concentration of about 1.5×10^{17} cm^{-3} is found at a point halfway through the film. An apparent increase in Si is seen near the surface, although this could be an artifact due to charging effects in the SIMS measurement. Near the SiC/GaN interface a sharp increase in the Si concentration is found. This may indicate a buildup in the Si near the interface, although some uncertainty exists in this interpretation since the ions may be sputtering the film nonuniformly (*i.e.* due to the dislocations in the film) resulting in a premature signal from the substrate. In any case, it is clear that a substantial Si concentration exists in the films, and this can produce the observed n-type back-

ground carrier concentration.

As discussed above, nearly all the films we have grown and characterized were prepared using the *in situ* Si-cleaning step to remove the surface oxide formed during transfer from the H-etching apparatus and the MBE system. It is possible that the Si seen in the films arises from the excess 1/3 ML of Si which is left on the surface after this cleaning step; the amount of Si observed in the SIMS profiles is roughly consistent with this mechanism. To test this possibility, we have prepared several films *without* using the Si-cleaning step, either by overgrowing on MOCVD-grown GaN or by growing on sapphire (the latter yielding N-polar material [11]). We find in this case background carrier concentrations which are 3–10 times lower than for the samples prepared with Si-cleaning, indicating that excess Si in those samples is indeed arising from the Si-cleaning procedure.

6 Optical Characterization

A typical low-temperature PL spectrum obtained from our GaN films is shown in Fig. 9, obtained from a sample grown with Ga/N flux ratio of about 1.6. An intense donor bound exciton (DBE) line, (D0,X), at 3.47 eV is seen, with FWHM of 10 meV. Donor-acceptor (D-A) features are seen in the range 3.1–3.3 eV, and deep luminescence bands are seen near 2.8 eV (blue luminescence, BL) and 2.2 eV (yellow luminescence, YL). We tentatively associate the 2.8 eV band with intrinsic defects such as N vacancies, as seen in Mg-containing material [20], although we do note the similarity of this band with one previously reported in GaN films and attributed to D-A transitions in the SiC substrates [21]. The 2.2 eV band is commonly observed in GaN prepared under a broad range of conditions. A set of weak lines is seen in the range 3.33–3.43 eV, as shown in the inset of Fig. 9. The line at 3.40 eV has been associated with oxygen in GaN [22]. In our case, we find for our early films which were grown without a nitrogen purifier (see Section II) that this line was always observed and it sometimes had a large intensity comparable to the DBE. Later films, grown with the nitrogen filter, show no evidence of this line, thus supporting its interpretation as arising from oxygen (O). The set of lines centered near 3.35 eV have been associated with stacking faults (SF) near the GaN/SiC interface [23].

Figure 10 shows the effect of substrate preparation on the spectra. The spectrum in Fig. 10(a) is identical to that of Fig. 9. Figure 10(b) shows a spectrum obtained from a sample for which the H-etching procedure was not used but the Si-cleaning of the substrate was performed. This spectrum shows different D-A features than those of our other films, suggestive of a different impurity concentration in the sample (the H-etching removes the top ~ 150 nm of the SiC, thereby removing impurities from the surface as well). As discussed in Section IV and shown in Fig. 6(b), this sample has numerous stacking faults which define small regions of cubic stacking near the GaN/SiC interface. The spectrum in Fig. 10(b) shows a clear set of SF lines near 3.35 eV, which, at least compared to the D-A luminescence have greater intensity that those of Fig. 10(a). Figure 10(c) shows a spectrum obtained from a film grown without H-etching or Si-cleaning. TEM results from this sample (not shown) indicated very poor structural quality, with numerous dislocations and stacking faults, and large regions of cubic stacking in the material. The spectrum shows intense DBE and D-A pair lines from cubic GaN [24].

Figure 11 shows the influence of the Ga/N flux ratio on the spectra, particularly for the deep luminescence. We consistently find that as this flux ratio is increased, the BL feature near 2.8 eV

shows greater intensity relative to the 2.2 eV YL. This result is consistent with the expectation of N vacancy formation under very Ga rich conditions. We also note that the width of the DBE increases with increasing Ga/N ratio, and for the least Ga rich conditions (bottom spectrum) we see an indication of a free exciton shoulder, F_X^A, at 3.48 eV. The spectra in Fig. 11 were all acquired using He-Cd excitation. An intense line at 3.448 eV is seen in the spectra, and from comparison with similar spectra acquired with frequency-doubled Ar laser excitation we can identify this feature as arising from the He-Cd laser line which is Raman shifted by multiple GaN longitudinal-optical phonon energies, in agreement with the identification of Dewsnip *et al.* [25] .

7 Summary

In summary, we find that the use of appropriate substrate preparation and growth conditions for GaN on SiC heteroepitaxy can lead to material of relatively high structural quality. H-etching of the substrate is important to eliminate stacking disorder in the GaN, and high growth temperature reduces the density of screw dislocations in particular. The mechanisms underlying the dislocation formation and annihilation are fairly well understood. A background electron concentration in the mid-10^{17} cm^{-3} range is found in the films, and is tentatively attributed to Si donors arising from the Si-cleaning step (used to remove surface oxide formed during the sample transfer between the H-etching apparatus and the MBE chamber).

Discussions with O. Brandt and J. S. Speck are gratefully acknowledged. This work was supported in part by the Office of Naval Research (grants N00014-96-1-0214, N00014-96-1-0333, and N00014-99-1-1067), the Air Force Office of Scientific Research (grant F33615-95-C-1619), and the National Science Foundation (grant DMR-9985898).

[1] B. Heying, X. H. Wu, S. Keller, Y. Li, D. Kapolnek, B. P. Keller, S. P. DenBaars, and J. S. Speck, Appl. Phys. Lett. **68**, 643 (1996).

[2] D. Kapolnek, S. Keller, R. Vetury, R. D. Underwood, P. Kozodoy, S. P. DenBaars, and U. K. Mishra, Appl. Phys. Lett. **71**, 1204 (1997).

[3] O.-H. Nam, M. D. Bremer, T. S. Zheleva, and R. F. Davis, Appl. Phys. Lett. **71**, 2638 (1997).

[4] V. Ramachandran, M. F. Brady, A. R. Smith, R. M. Feenstra, and D. W. Greve, J. Electron. Mater. **27**, 308 (1998).

[5] V. Ramachandran, A. R. Smith, R. M. Feenstra, and D. W. Greve, J. Vac. Sci. Technol. A **17**, 1289 (1999).

[6] V. M. Torres, J. L. Edwards, B. J. Wilkens, D. J. Smith, R. B. Doak, and I. S. T. Tsong, Appl. Phys. Lett. **74**, 985 (1999).

[7] Q. Z. Xue, Q. K. Xue, Y. Hasegawa, I. S. T. Tsong, and T. Sakurai, Appl. Phys. Lett. **74**, 2468 (1999).

[8] R. Lantier, A. Rizzi, D. Guggi, H. Lüth, B. Neubauer, D. Gerthsen, S. Frabboni, G. Colì, and R. Cingolani, MRS Internet J. Nitride Semicond. Res. **4S1**, G3.50 (1999).

[9] O. Brandt, R. Muralidharan, P. Waltereit, A. Thamm, A. Trampert, H. von Kiedrowski, and K. H. Ploog, Appl. Phys. Lett. **75**, 4019 (1999).

[10] E. J. Tarsa, B. Heying, X. H. Wu, P. Fini, S. P. DenBaars, and J. S. Speck, J. Appl. Phys. **82**, 5472 (1997).

[11] A. R. Smith, V. Ramachandran, R. M. Feenstra, D. W. Greve, A. Ptak, T. H. Myers, W. L. Sarney, L. Salamanca-Riba, M.-S. Shin, and M. Skowronski, MRS Internet J. Nitride Semicond. Res. **3**, 12 (1998).

[12] V. Ramachandran and R. M. Feenstra, Phys. Rev. Lett. **82**, 1000 (1999).

[13] C. Youtsey, L. T. Romano, R. J. Molnar, and I. Adesida, Appl. Phys. Lett. **74**, 3537 (1999).

[14] A. Sagar, C. D. Lee, and R. M. Feenstra, unpublished.

[15] B. W. Dodson and J. Y. Tsao, Appl. Phys. Lett. **51**, 1325 (1987).

[16] W. L. Sarney, L. Salamanca-Riba, V. Ramachandran, R. M. Feenstra, and D. W. Greve, MRS Internet J. Nitride Semicond. Res. **5S1**, W3.47 (2000).

[17] V. Ramachandran, R. M. Feenstra, W. L. Sarney, L. Salamanca-Riba, and D. W. Greve, J. Vac. Sci. Technol. A, Jul/Aug (2000), to appear.

[18] P. Fini, X. Wu, E. J. Tarsa, Y. Golan, V. Srikant, S. Keller, S. P. DenBaars, and J. S. Speck, Jpn. J. Appl. Phys. **37**, 4460 (1998).

[19] J. Elsner, Th. Frauenheim, M. Haugk, R. Gutierrez, R. Jones, and M. E. Heggie, MRS Internet J. Nitride Semicond. Res. **4S1**, G3.29 (1999).

[20] U. Kaufmann, M. Kunzer, M. Maier, H. Obloh, A. Ramakrishnan, B. Santic, and P. Schlotter, Appl. Phys. Lett. **72**, 1326 (1998).

[21] O. Brandt, B. Yang, H.-J. Wünsche, U. Jahn, J. Ringling, G. Paris, H. T. Grahn, and K. H. Ploog, Phys. Rev. B **58**, R13407 (1998).

[22] J. M. Hayes, M. Kuball, A. Bell, I. Harrison, D. Korakakis, and C. T. Foxon, Appl. Phys. Lett. **75**, 2097 (1999).

[23] W. Rieger, R. Dimitrov, D. Brunner, E. Rohrer, O. Ambacher, and M. Stutzmann, Phys. Rev. B **54**, 17596 (1996).

[24] J. Menniger, U. Jahn, O. Brandt, H. Yang, and K. Ploog, Phys. Rev. B **53**, 1881 (1996).

[25] D. J. Dewsnip, A. V. Andrianov, I. Harrison, D. E. Lacklison, J. W. Orton, J. Morgan, G. B. Ren, T. S. Cheng, S. E. Hooper, and C. T. Foxon, Semicond. Sci. and Technol. **12**, 55 (1997).

TABLE I. Values for the FWHM of triple-axis XRD lines, and the density of threading dislocations (TD) which intersect the surface.

	FWHM (arcsec)		TD density (cm^{-2})
This work	25	[(ω-2θ (0002)]	$\approx 1\times10^{9}$ (edge)
(MBE)	60	[ω (0002)]	$< 1\times10^{6}$ (screw)
	75	[ω-2θ($10\bar{1}4$)]	
	470	[ω ($10\bar{1}4$)]	
Brandt et al.	25	[ω-2θ (0002)]	$< 10^{9}$ (total)
(MBE,	100	[ω (0002)]	
Ref. [9])	-	[ω-2θ ($10\bar{1}3$)][a]	
	300	[ω ($10\bar{1}3$)][b]	
Heying et al.	23	[ω-2θ (0002)]	4×10^{8} (edge)
(MOCVD,	269	[ω (0002)]	4×10^{8} (screw
Ref. [1])	54	[ω-2θ($10\bar{1}2$)]	or mixed)
	413	[ω ($10\bar{1}2$)]	

a not reported

b O. Brandt, private communication

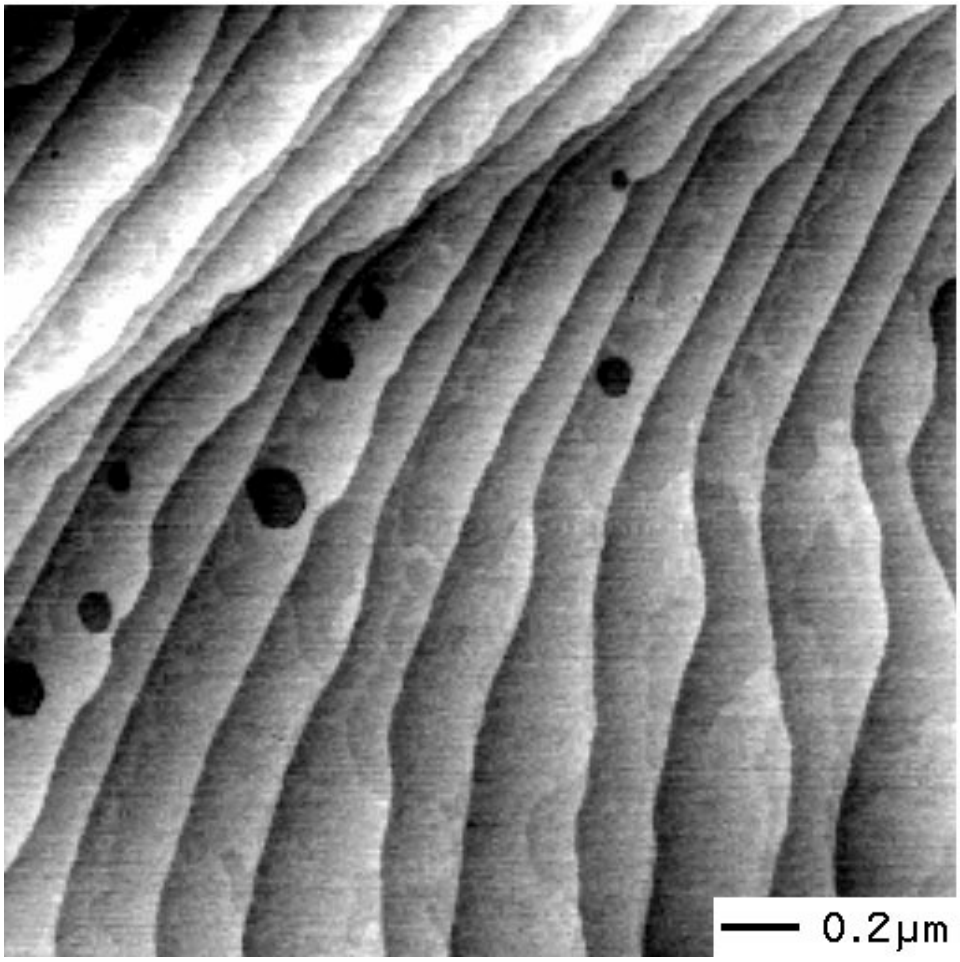

Figure 1 AFM image of SiC(0001) surface following the Si-cleaning step. All observed steps have a height of 7.5 Å (the small hexagonal pits are also 7.5 Å deep). Grey-scale range is 15 Å.

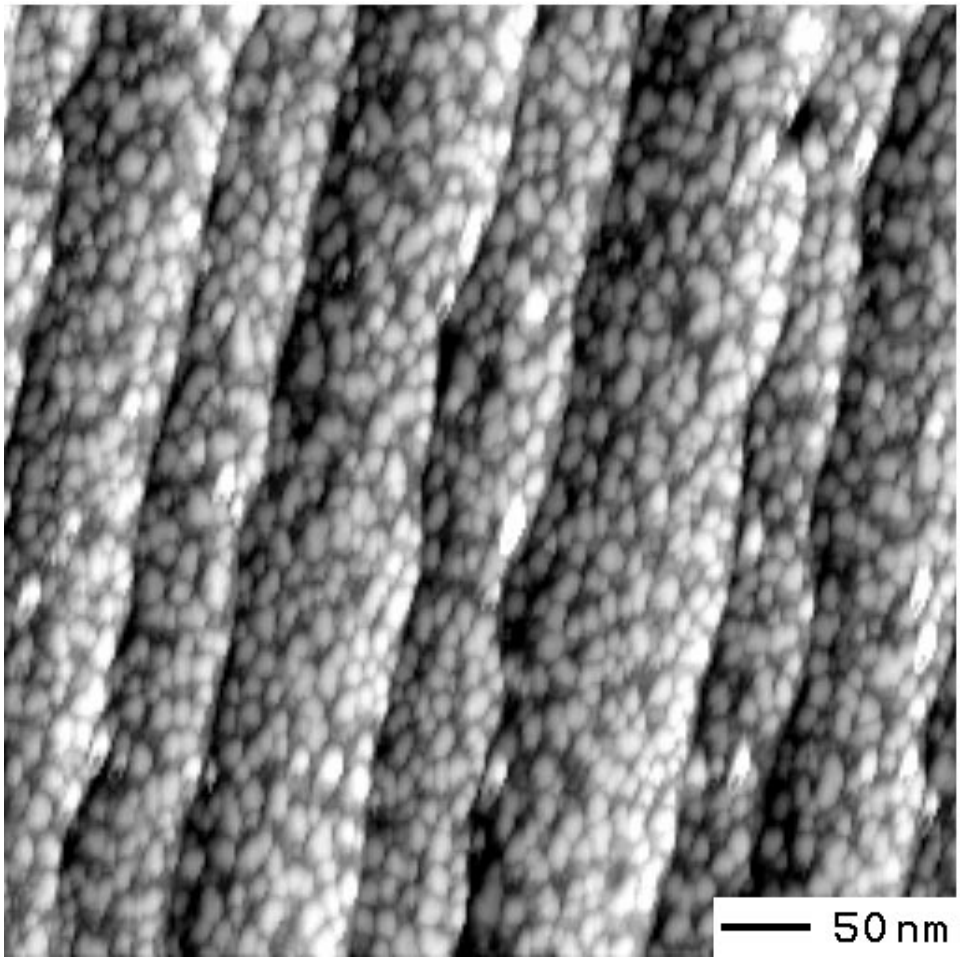

Figure 2 STM image showing nucleation of GaN on SiC(0001). Average GaN thickness is 0.3 ML. Growth temperature is 650° C. Grey-scale range is 12 Å.

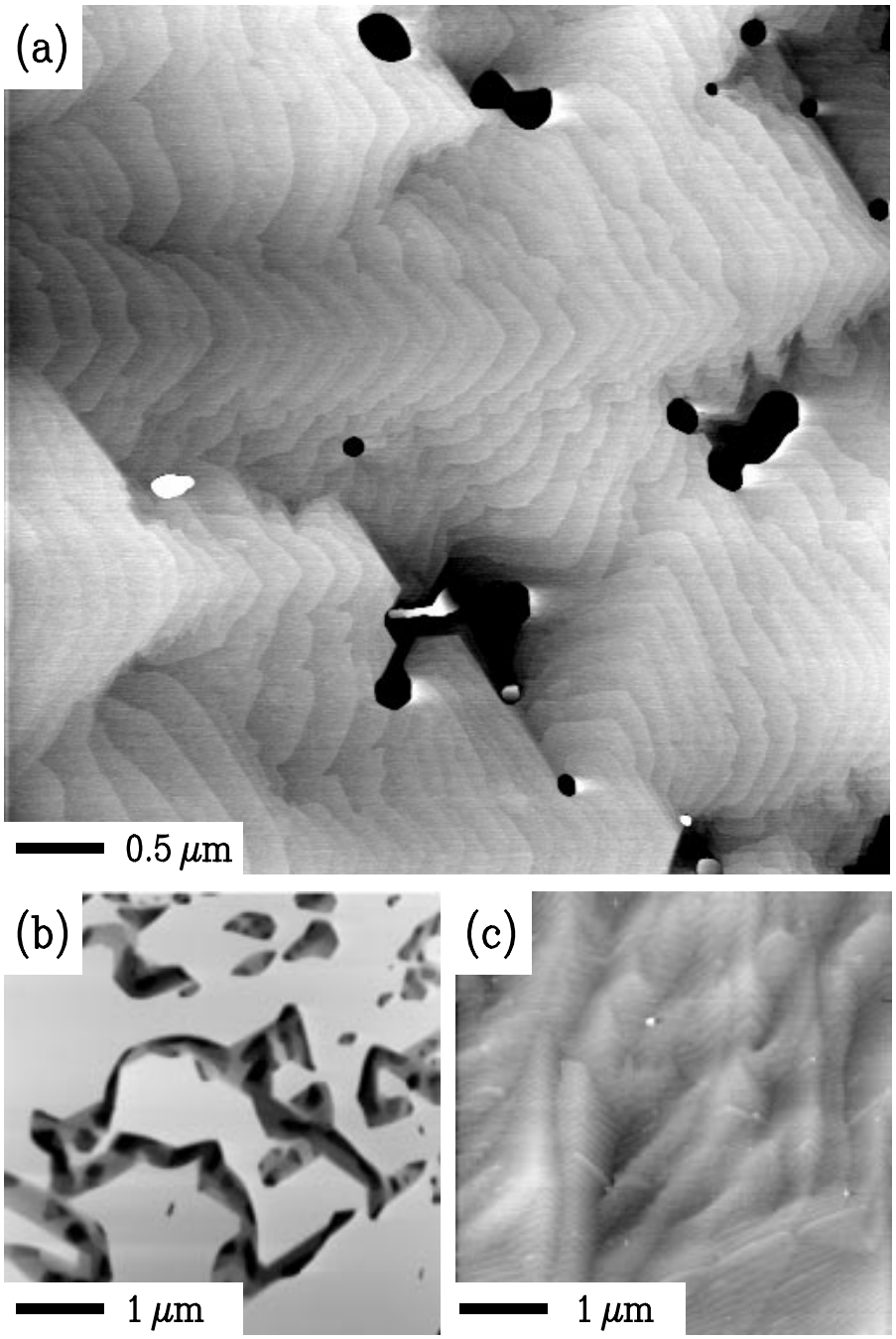

Figure 3 AFM images of GaN(0001) film grown at 750° C on H-etched 6H-SiC, with Ga/N flux ratios of (a) 1.3, (b) 1.1, and (c) 1.6. Pits on the surface are seen in (a), arising from dislocations. The grey-scale ranges are 5 nm, 86 nm, and 5 nm for (a)–(c) respectively.

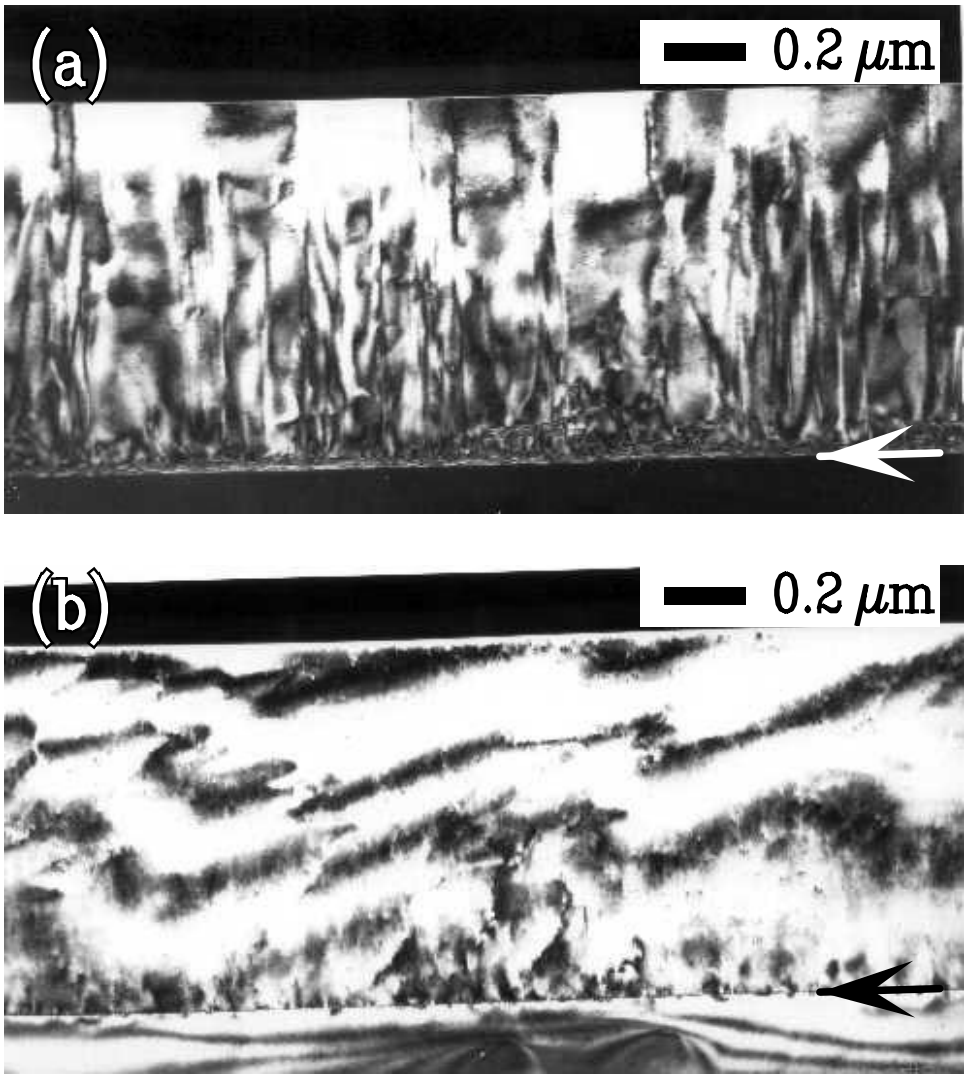

Figure 4 (a) and (b) Dark field two-beam TEM images of GaN films grown on H-etched 6H-SiC(0001), (a) g=[01$\bar{1}$0] and (b) g=[0002]. Arrows mark the GaN/SiC interface.

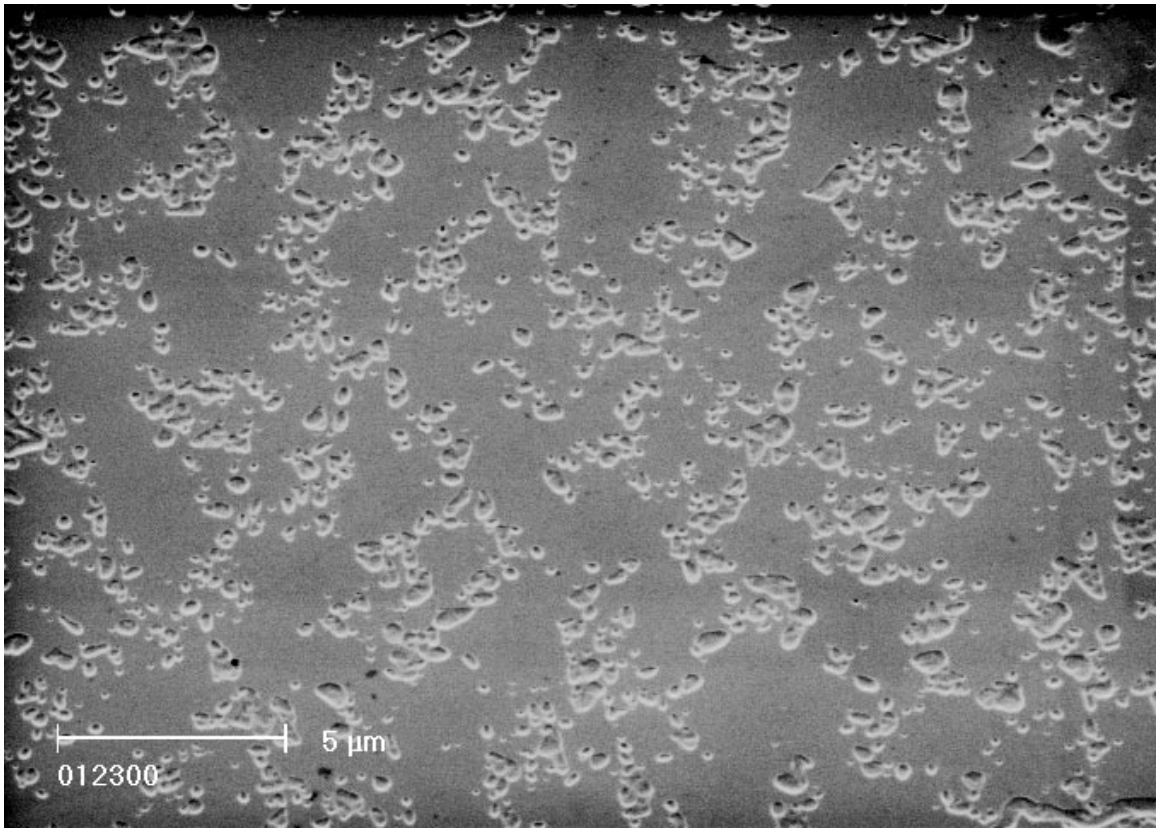

Figure 5 SEM image of GaN film, grown at 750° C, which has been photoelectrochemically etched to reveal the dislocations. The scale bar corresponds to a length of 5 µm.

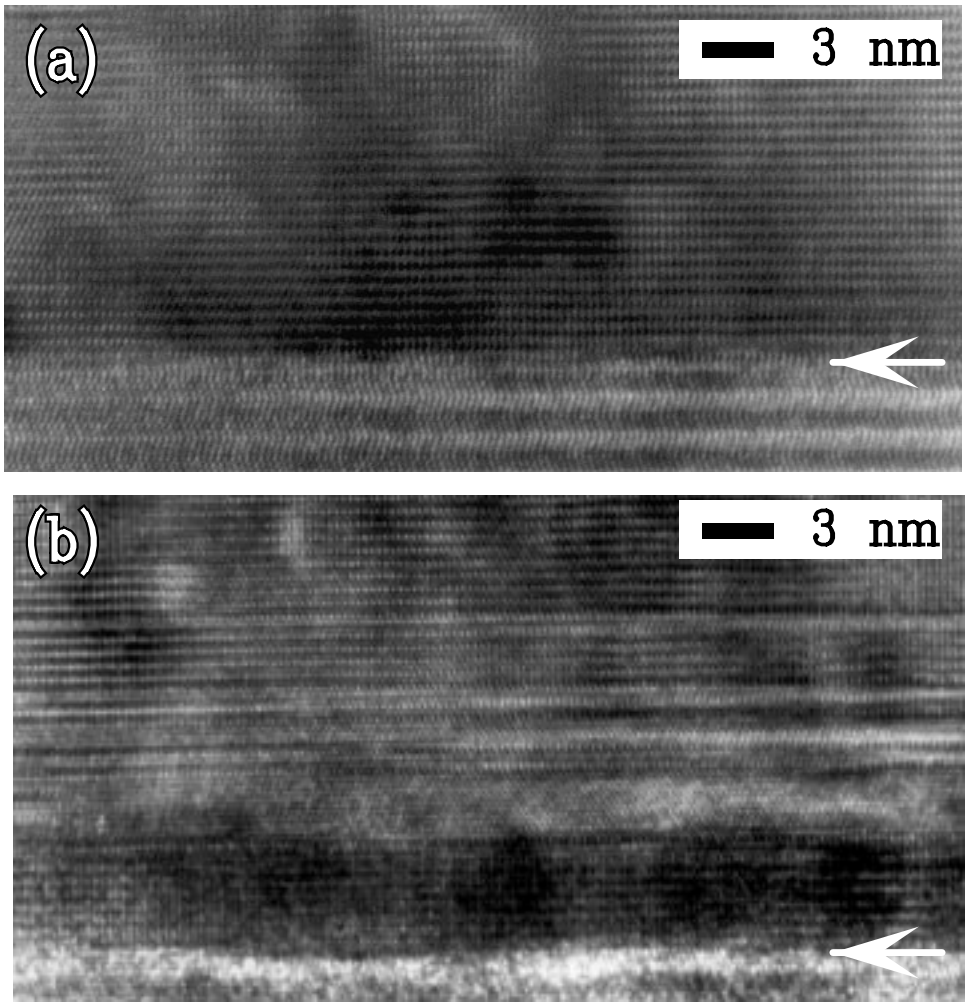

Figure 6 High resolution TEM image of GaN on 6H-SiC(0001) prepared (a) with and (b) without H-etching. Zone axis is [$2\bar{1}10$]. Arrows mark the GaN/SiC interface.

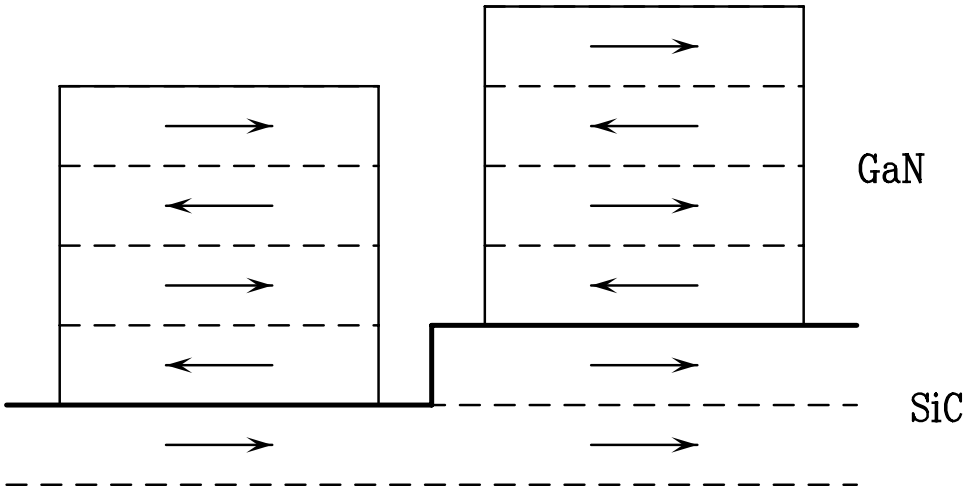

Figure 7 Stacking sequence for GaN layers on SiC, illustrating the manner in which a single bilayer step in the SiC produces oppositely oriented GaN grains on the two terraces.

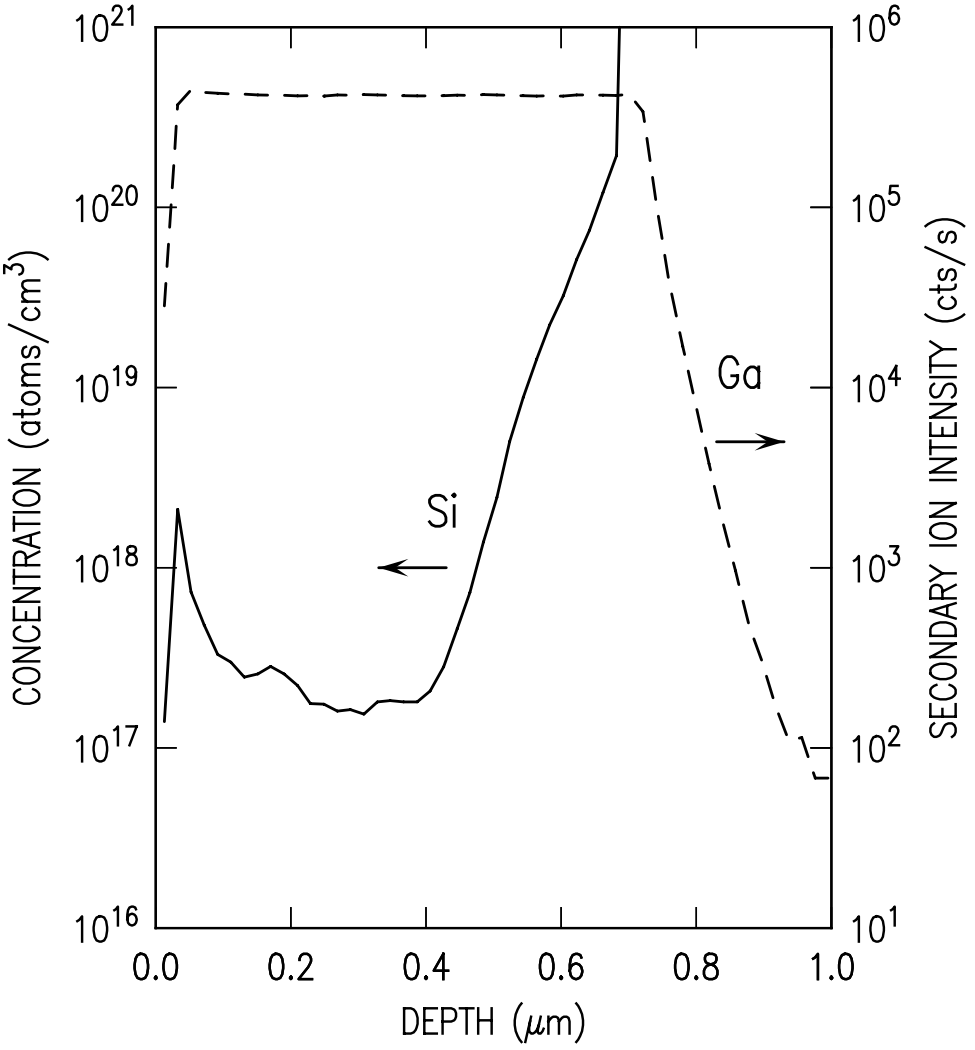

Figure 8 SIMS profile of Ga and Si concentration in 0.6 μm thick GaN film grown on SiC at 750° C, using H-etching and Si-cleaning of the SiC.

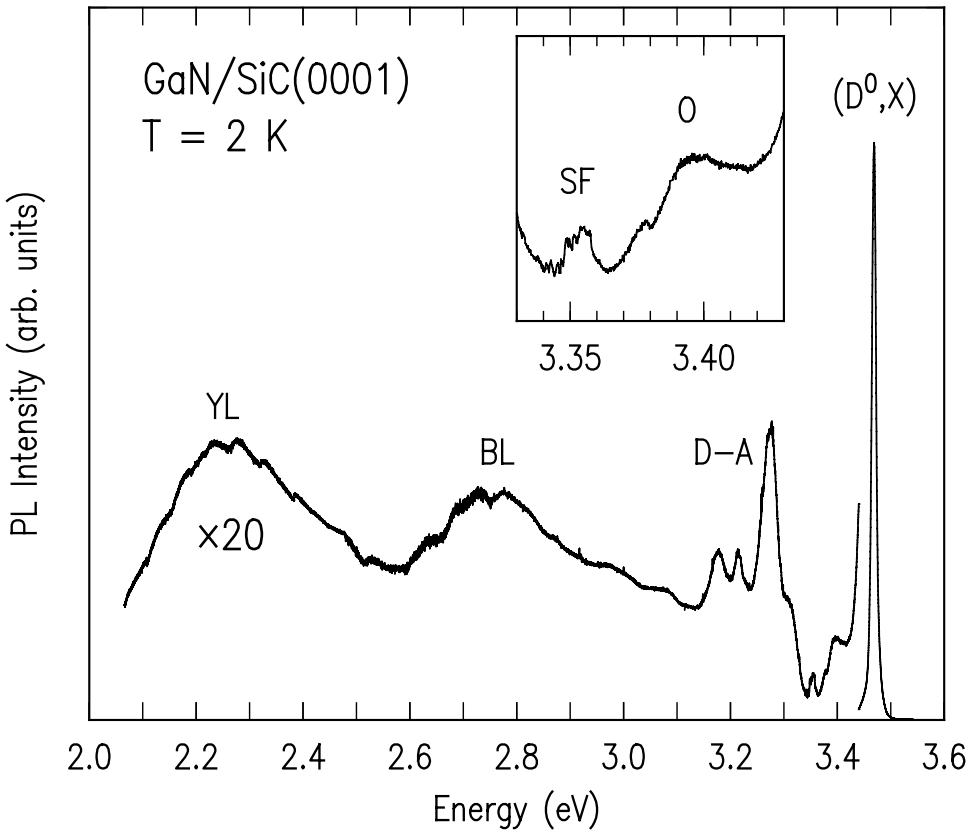

Figure 9 PL spectrum for GaN films grown with Ga/N flux ratio of 1.6 and at growth temperature of 750° C. Inset shows an expanded view of the spectral region from 3.3–3.4 eV.

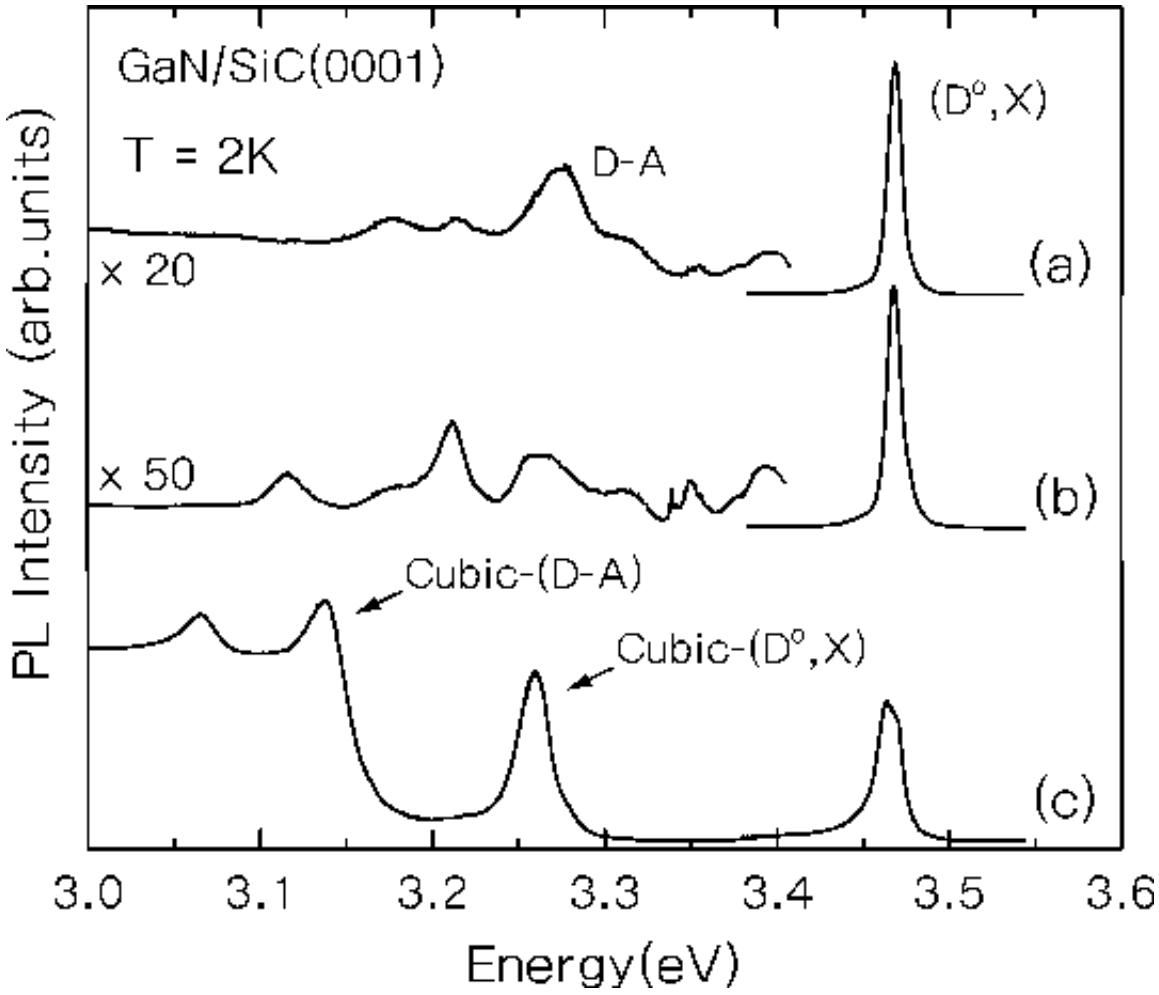

Figure 10 Comparison of PL spectra for samples prepared under different conditions; (a) standard growth using H-etching and Si-cleaning, (b) without H-etching, (c) without both H-etching and Si-cleaning.

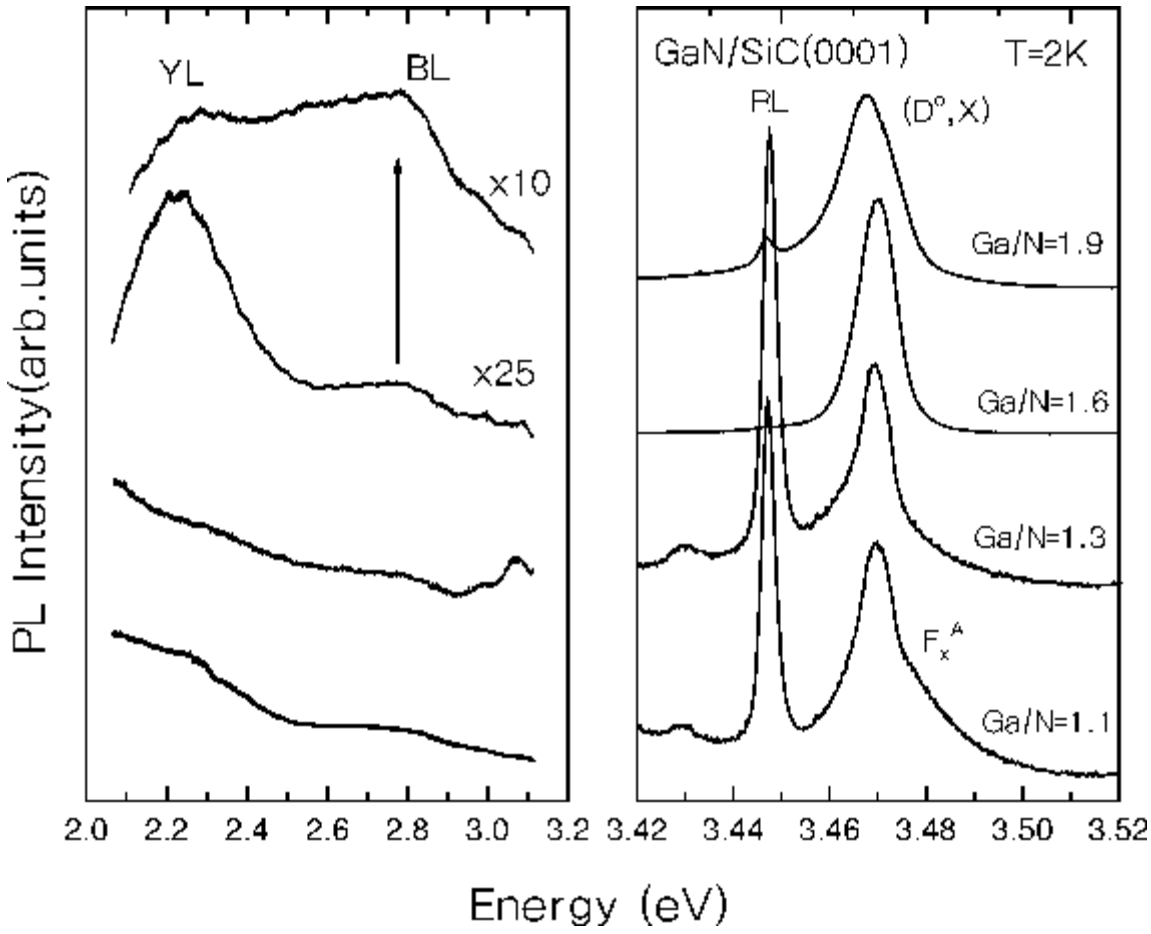

Figure 11 Comparison of PL spectra as a function of Ga/N flux ratio.